land

Article

Mapping and Quantification of Miombo Deforestation in the Lubumbashi Charcoal Production Basin (DR Congo): Spatial Extent and Changes between 1990 and 2022

Héritier Khoji Muteya [1,2,*] , Dieu-donné N'Tambwe Nghonda [1,2] , Franco Mwamba Kalenda [3],
Harold Strammer [2], François Munyemba Kankumbi [1], François Malaisse [2], Jean-François Bastin [2],
Yannick Useni Sikuzani [1] and Jan Bogaert [2,4,*]

1   Unité Ecologie, Restauration Ecologique et Paysage, Faculté des Sciences Agronomiques, Université de Lubumbashi, Lubumbashi BP 1825, Democratic Republic of the Congo; nghondan@unilu.ac.cd (D.-d.N.N.); kankumbim@unilu.ac.cd (F.M.K.); sikuzaniu@unilu.ac.cd (Y.U.S.)
2   Unité Biodiversité et Paysage, Université de Liège—Gembloux Agro-BioTech, 5030 Gembloux, Belgium; harold.strammer@uliege.be (H.S.); malaisse1234@gmail.com (F.M.); jfbastin@uliege.be (J.-F.B.)
3   Unité Évaluation de L'aptitude des Terres et Agrométéorologie, Faculté des Sciences Agronomiques, Université de Lubumbashi, Lubumbashi BP 1825, Democratic Republic of the Congo; kalendaf@unilu.ac.cd
4   Ecole Régionale Post-Universitaire d'Aménagement et de Gestion Intégrés des Forêts et Territoires Tropicaux (ERAIFT), Université de Kinshasa (UNIKIN), Kinshasa BP 15373, Democratic Republic of the Congo
*   Correspondence: khoji.muteya@unilu.ac.cd (H.K.M.); j.bogaert@uliege.be (J.B.)

Abstract: Population growth in the city of Lubumbashi in the southeastern Democratic Republic of the Congo (DR Congo) is leading to increased energy needs, endangering the balance of the miombo woodland in the rural area referred to as the Lubumbashi charcoal production basin (LCPB). In this study, we quantified the deforestation of the miombo woodland in the LCPB via remote sensing and landscape ecology analysis tools. Thus, the analysis of Landsat images from 1990, 1998, 2008, 2015 and 2022 was supported by the random forest classifier. The results showed that the LCPB lost more than half of its miombo woodland cover between 1990 (77.90%) and 2022 (39.92%) and was converted mainly to wooded savannah (21.68%), grassland (37.26%), agriculture (2.03%) and built-up and bare soil (0.19). Consecutively, grassland became the new dominant land cover in 2022 (40%). Therefore, the deforestation rate (−1.51%) is almost six-times higher than the national average (−0.26%). However, persistent miombo woodland is characterised by a reduction, over time, in its largest patch area and the complexity of its shape. Consequently, because of anthropogenic activities, the dynamics of the landscape pattern are mainly characterised by the attrition of the miombo woodland and the creation of wooded savannah, grassland, agriculture and built-up and bare soil. Thus, it is urgent to develop a forest management plan and find alternatives to energy sources and the sedentarisation of agriculture by supporting local producers to reverse these dynamics.

Keywords: anthropogenic pressure; charcoal; miombo woodland; landscape ecology; GIS/remote sensing

1. Introduction

Forests provide numerous benefits to rural communities and society as a whole [1]. Specifically, forests serve as a source of food, medicine, fuel wood, income and employment for millions of rural inhabitants, supporting their livelihoods and improving food security in less developed countries [2,3]. Forests also offer important environmental benefits, such as regulating the air and water, facilitating crop pollination, improving soil fertility and reducing erosion [4,5]. Because of overexploitation, forests are under significant anthropogenic pressure, which leads to habitat loss and fragmentation [6,7]. For instance, globally, 2.3 million square kilometres of forest were destroyed between 2000 and 2012 [8]. Habitat loss and fragmentation are leading to biodiversity loss and compromising the ecosystem services provided by forest ecosystems [9,10].

Deforestation and degradation are a particular concern for tropical forests as they host a substantially high proportion of global biodiversity [7,8]. On average, 9.28 million hectares of these forests was destroyed annually between 2015 and 2020 [11]. For example, the Amazon has experienced a loss of at least 17% of its primary forests in the past 50 years [12], while in Southeast Asia, logging resulted in the loss of approximately 1.1 million hectares between 2000 and 2020 [13].

Africa is known for having some of the most productive and biomass-dense forests globally. However, it is continuously under deforestation threat, owing to rising demands for timber and wood energy, particularly owing to Africa's growing population [14]. The loss of 3.9 million hectares of forest between 2010 and 2020 signifies the urgency of this issue [11]. In the Congo Basin, the deforestation rate increased from 0.09% between 1990 and 2000 to 0.17% between 2000 and 2005, mainly owing to the loss of forest in the Democratic Republic of the Congo (DR Congo). Indeed, the DR Congo has nearly 23% of Africa's forests [15], yet it experienced a deforestation rate increase from 0.11% between 1990 and 2000 to 0.22% between 2000 and 2005 [16]. However, political unrest, corruption and poor governance have fostered unregulated resource exploitation, including timber extraction, charcoal production and artisanal mining [17]. These factors are linked to agriculture, which is commonly regarded as the primary cause of deforestation and degradation [18,19].

The DR Congo is home to 145 million hectares of forest, including dense rainforest, mountain forests, woodland (such as miombo woodland) and the savannah–forest mosaic [19]. The miombo woodland, which covers 11% of the national territory, is particularly abundant in the southeast, particularly in the Upper Katanga Province, a region known for mining [20,21]. Unfortunately, this mining region has experienced significant fragmentation and loss of miombo woodland cover, mainly around agglomerations, including the city of Lubumbashi [22–26].

Since its creation in 1910, Lubumbashi, the DR Congo's second-largest city in terms of population and economic capital, has been mostly covered by miombo woodland [27]. The growth of its internal population, combined with an exodus, has led to uncontrolled urban sprawl since the country's political independence in 1960 [25,28]. This demographic pressure is now one of the leading causes of deforestation, as most households depend on the forest for timber, construction wood and, particularly, fuel wood for energy [29]. In Lubumbashi, electricity production and distribution are inadequate to meet the needs of the population, which surpassed 3 million inhabitants in 2020 [30]. As a result, charcoal has become the primary domestic energy source, meeting the demands of over 72% of households [29].

Thus, the pressure on the miombo woodlands from slash-and-burn agriculture and charcoal production around Lubumbashi [29] has altered the landscape patterns. Currently, analysing changing landscape trends is facilitated by readily available satellite imagery sources and various machine learning techniques for image classification [31]. Several studies have examined the landscape dynamics in the Katanga region, particularly in the Lubumbashi area, using satellite imagery [22–24,32–39]. However, none have reported the dynamics of landscape anthropisation in the Lubumbashi charcoal production basin (LCPB). Given the dependency of the urban population on miombo wood for charcoal, particular attention needs to be focused on the LCPB. Indeed, landscape pattern dynamics from anthropogenic or natural factors, consequently, modify the ecological functioning of landscapes, which can be determined via an assessment of their ecosystem properties and services.

In this study, we quantified the miombo deforestation and degradation evolution within the LCBP. We hypothesised that it is decreasing directly because of charcoal production and agriculture and indirectly because of a lack of territorial planning. This situation is reflected in the decreasing number of patches and areas of miombo cover in the LCBP relative to the increasing values of the number of patches and areas for anthropogenic land cover, such as for savannahs, fields and infrastructure. We also verified that the deforestation rate in the LCBP is higher than the national average.

2. Materials and Methods

2.1. Research Area

The LCPB is located in the Upper Katanga Province in the southeastern part of the DR Congo (10°39′7.47″–12°26′37.61″ S and 26°20′54.95″–28°40′13.55″ E), covering an area of 26,603.4 km². The limits of the LCPB were highlighted after a semi-structured survey conducted in the city of Lubumbashi between February and July 2021. Fourteen charcoal storage sites were investigated to determine the origin of the charcoal from a total of 150 respondents interviewed (10 and 20 individuals per charcoal storage site) using the Raosoft.com tool supported by the Bernoulli sampling equation [40]. Thus, sixty-three villages, covering five administrative sectors, were cited as sources of charcoal sold in the city of Lubumbashi. The LCPB covers all the administrative sectors from which the city of Lubumbashi is supplied with charcoal (Figure 1).
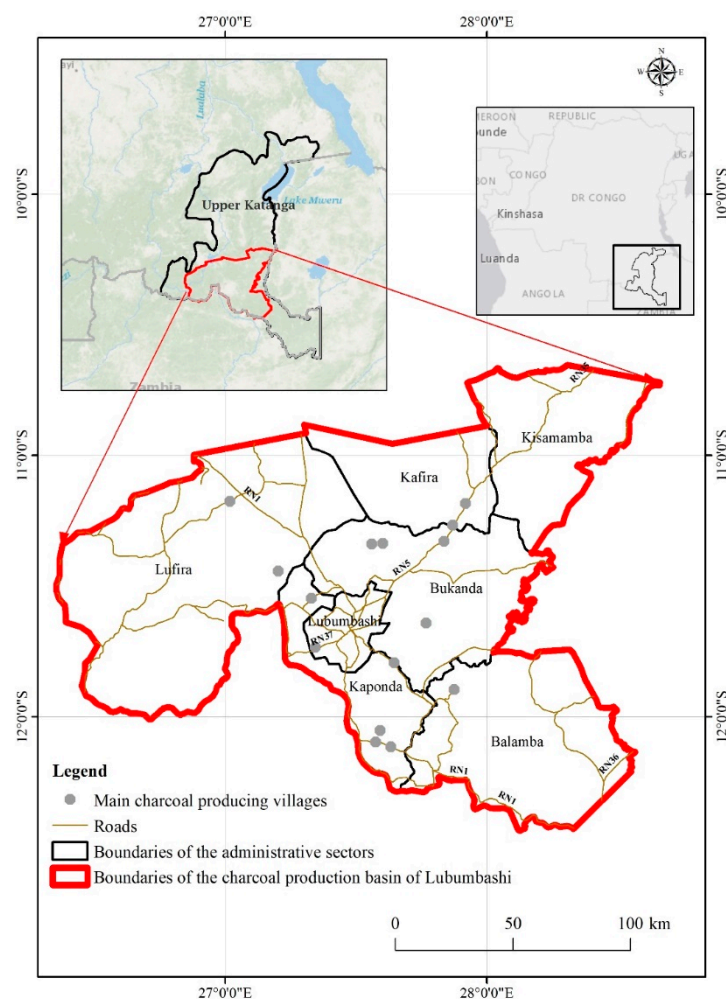
Figure 1. Geographic location of the Lubumbashi charcoal production basin (LCPB), comprising charcoal-producing villages located in the Kaponda, Bukanda, Balamba, Lufira and Kisamamba sectors of Upper Katanga Province in the DR Congo. The roads shown are the main axes that facilitate the evacuation of charcoal, which amplifies deforestation.

The LCPB has an average altitude of 1200 to 1300 m and is classified as having a Cw climate according to Köppen's classification, with a rainy season (November–March), a dry season (May–September) and two transitional months (April and October) [41]. Ref. [42] defined five seasons based on phenological observations of vegetation: the cold dry season (May–July), the hot dry season (August–September), the early rainy season (October–November), the full rainy season (December–February) and the late rainy season (March–April). The average annual rainfall is 1200 mm, and a trend towards later onset

of rain and lower average annual rainfall has been observed [27,43]. In the latter half of the 20th century, the annual average temperature was 20 °C, but recent warming has been observed [43]. Vegetation around Lubumbashi (and in the LCPB in general) is covered by open forest (*miombo* in the local language), dense dry forest (*muhulu* in the local language), gallery forest (*mushitu* in the local language) and variations of savannah and marshy grasslands [27]. The natural wooded vegetation, currently in fragmented form, is located several kilometres from Lubumbashi and is frequently replaced by savannah [22,35,42]. Ferralsols are the most dominant type of soil in this region [44]. Populations depend mainly on shifting agriculture, charcoal production, artisanal logging and the exploitation of non-timber forest products [19]. The rare actions of provincial government departments and non-governmental organisations in mitigating deforestation caused by these activities are focused on the implementation of simple management plans, reforestation and forest control [40].

2.2. Acquisition and Processing of Satellite Data

2.2.1. Source of Satellite Data

The LCPB was isolated from Landsat images of TM (Thematic Mapper) sensor (1990, 1998 and 2008), OLI-TIRS-1 (2015) and OLI-TIRS-2 (2022) of a 30 m spatial resolution. Specifically, the year 1990 saw the democratisation of the country, accompanied by various socio-political crises, exacerbating the poverty of the urban population. The year 1998 was, therefore, chosen to observe the impact of the change in the country's political vision, characterised by strong decentralisation of power, on the dynamics of the forest landscape. Overall, the 1990–1998 period also corresponds to the period before the liberalisation of the mining sector. Liberalisation of the mining sector in 2002 led to significant demographic growth and urban spatial dynamics, the effects of which on the landscape could be seen in 2008 [28,36]. The year 2015 also saw the break-up of the former province of Katanga into 4 new provinces, including Upper Katanga, whose capital remains the city of Lubumbashi. This was followed by major foreign investment in the mining and infrastructure sectors, the effects of which on the landscape could be seen in 2022.

These images were downloaded and analysed on the Google Earth Engine (GEE) platform. The GEE provides free satellite imagery and large-scale spatial analysis and calculation functions, which can be used to assess spatiotemporal changes in the landscape pattern [45], as shown by several studies [20,45,46]. Furthermore, Landsat satellite images have the advantage of being low-cost and offering the potential to survey large areas despite their lower spatial resolution [47]. The images were acquired between June and July (during the dry season) to maintain consistency in the spectral response of the different vegetation covers [48].

2.2.2. Preprocessing of Landsat Images

The image with the minimum cloud (<10%) cover for each target year in the study area was selected as the data source to establish the sample dataset [49]. These Landsat images were reprojected into the WGS 84/UTM 35s system and mapped onto a pre-defined pixel grid using bilinear interpolation to facilitate subsequent image composition [20]. After radiometric correction, the images were cut and spliced, and the bands were synthesised [46]. The false-colour composite of Landsat images was created by combining the mid-infrared (MIR), near-infrared (NIR), red (R) and green (G) bands, with the second and the third bands allowing for the best discrimination of vegetation [50].

2.2.3. Supervised Classification of Landsat Images

For the supervised classification, six dominant land covers were identified in the LCPB: miombo woodland, wooded savannah, grassland, agriculture, built-up and bare soil and water (Table 1). Points for each land cover were identified on the false-colour composite image. The high-resolution image provided by GEE was also helpful for visual interpretation of the images [46]. The delineation and placement of these points and

polygons were removed from the edge zones to exclude mixed pixels [51]. These points were then combined into a single feature collection, which was subsequently used to collect training and validation data by sampling the input imagery [45]. The training data were used to drive the random forest algorithm, which creates decision trees that assign each pixel to the associated land cover [46,52]. The main parameters of a random forest classifier based on GEE include the number of classification trees, the number of variables in each classification tree, the minimum sample leaves, the input variables of a decision tree, out-of-bag (OOB) mode and the random seed sample data for the construction of the decision tree [49,53]. This method provides higher classification accuracy than other classification algorithms, such as the support vector machine (SVM), k-nearest neighbour (k-NN) and maximum likelihood classifier (MLC) [54,55].

2.2.4. Accuracy Assessment and Area Estimation

Samples were randomly stratified according to a map of 12 classes or strata for each period, with 6 stable classes (miombo woodland, wooded savannah, grassland, agriculture, built-up and bare soil and water) and 5 relevant classes of change. After applying Equation 5.25 from Ref. [56] to determine the sample size, we sampled 2000 points for 1990–1998, 2050 for 1998–2008, 2000 for 2008–2015 and 2100 for 2015–2022. Depending on the proportion of each stratum, 400 points were allocated to strata occupying more than 30%, 250 points were allocated to those occupying 20–30%, 200 points were allocated to those occupying 10–19%, 150 points were allocated to those occupying 1–9% and 100 points were allocated to those occupying less than 1%. The next step involved computing the error matrix expressed in terms of estimated area proportions. Adjustments were made to account for biases in the area and area change, which led to more precise estimates. To quantify the precision of area and changes in area estimates, we calculated the confidence intervals [57]. The measurement accuracies, including overall, user and producer accuracies, were computed using Equations (1)–(3) from Ref. [57]. Error-adjusted area estimates for each class and the standard error of the estimate (calculated using a 95% confidence interval, obtained by multiplying the standard error by 1.96) were determined using Equations (10) and (11) from Ref. [57]. Then, the analysis of disagreement between the land cover map and the reference land cover was performed using Equations (2)–(5) from Ref. [58], which allowed for computing the quantity disagreement (QD), relating to less-than-perfect match in land cover proportions, and allocation disagreement (AD), which relates to the less-than-optimal match in spatial allocation of land cover [59].

Table 1. Description of the land cover types for supervised classification of the landscape of the LCPB using the random forest classifier and points used as training data. The small images are Quick Bird images available free of charge on Google Earth from June 2022.
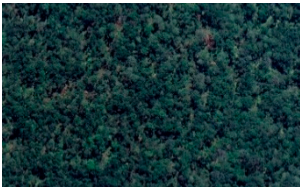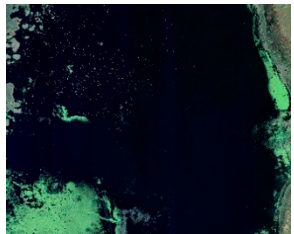
Land Cover Class	Description
Miombo woodland	Vegetation formation dominated by a sparse herbaceous layer under a 10–20-m-high forest stand. This is land in which tree cover predominates with a threshold canopy cover of a minimum of 10–30% and an area minimum of 0.05–1.0 hectares [60]. The miombo woodland is the dominant vegetation type in the Zambezian region, characterised by the majority of species belonging to the genera *Brachystegia*, *Julbernardia* and *Isoberlinia*.
Wooded savannah	Wooded savannah represents a transition between the open forest and the dembo (periodically flooded savannah) and corresponds to unfavourable edaphic conditions. In addition to this category, there are derived savannahs, which now replace many degraded open forests [27].

Table 1. *Cont.*

Land Cover Class	Description
Grassland	This land cover includes steppe savannahs and the dembo [27]. Although there are some natural savannas, the majority are the result of anthropogenic activities in the region. As a result, their presence in the landscape increases with the extent of anthropogenic activity.
Agriculture	Parcels cultivated and farmland that can be cultivated normally in ordinary years or put in rest to be cleared after a few years in a crop rotation system.
Built-up and bare soil	Bare land with sparse vegetation and a soil background. Residential land with minimal vegetation, impervious surfaces or rarely paved roads. This land cover includes mining areas in the LCPB.
Water	Surface water, including rivers and water ponds

2.2.5. Assessment of Landscape Dynamics

- Composition dynamics of landscape

The spatiotemporal change between land cover types was quantified via the transition matrix [23,38], from which the stability index was calculated [34,61]. The extent of deforestation was determined using the periodic deforestation rate. The annual deforestation rate was obtained by dividing the periodic deforestation rate by the number of years between the two dates of the considered period [38].

The diversity of patches and their distribution in the landscape were assessed via Simpson's diversity index (SIDI) and Simpson's evenness index (SIEI), respectively, using FRAGSTATS 4.2, free software for the analysis of landscape structure that was developed by the United States Department of Agriculture Forest Service. The SIDI represents the probability that two randomly selected cells are of different patch types, and the SIEI measures the distribution of the area between patch types [62]. These indices vary between 0 and 1, with higher values indicating greater landscape diversity [62].

- Structural dynamics of landscape

Landscape dynamics were quantified using the number of patches and the class area, which are elementary metrics [63] that can be used to easily evaluate the landscape fragmentation phenomenon. Spatial transformation processes were identified using a decision tree (Figure 2) based on the comparison of class area, perimeter and number of patches before

and after landscape transformation [39,61,64]. Among these processes, anthropogenic land covers are characterised by aggregation, enlargement and shift. However, natural land cover is characterised by attrition, perforation, shrinkage, deformation, dissection and fragmentation [65]). The value of $t = 0.75$ was used to distinguish the fragmentation process from dissection, where values above 0.75 suggest dissection and those below or equal to 0.75 indicate fragmentation [66]. Finally, this analysis was completed by calculating the largest patch index, while the extent of landscape anthropisation was determined from the fractal dimension, a measure of landscape complexity and an index of the scale dependency of landscape pattern [32,65].
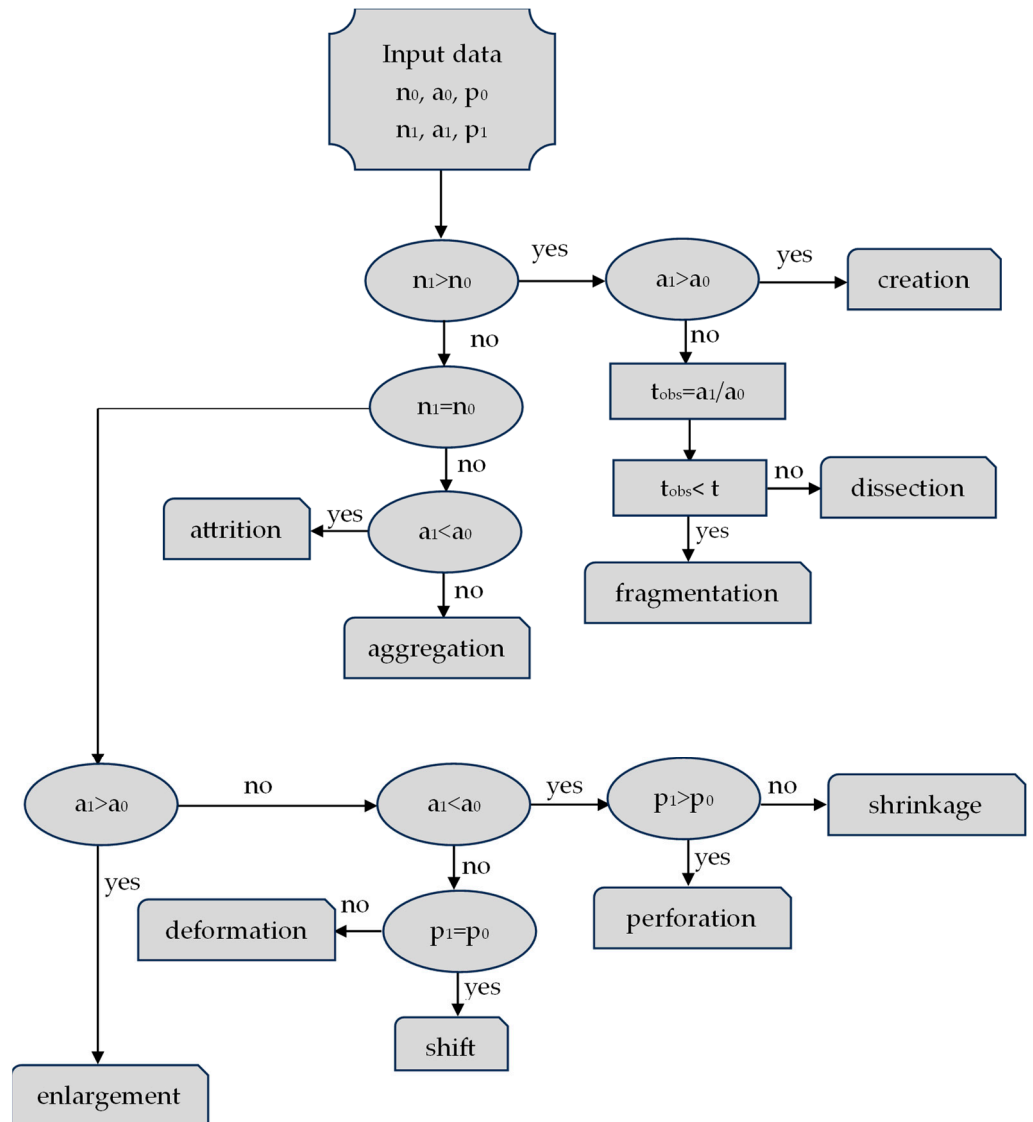
Figure 2. Decision tree used to identify the transformation processes that modify the spatial structure of landscapes. Parameters a_0, p_0 and n_0 refer to the area of the class, perimeter and number of patches before the transformation, respectively, and a_1, p_1 and n_1 refer to the reciprocal values after the change in spatial structure [61].

3. Results

3.1. Classification Validation and Land Cover Mapping

Tables 2–5 present the accuracy assessment and area estimate for stable land cover and land cover change maps from 1990 to 1998, 1998 to 2008, 2008 to 2015 and 2015 to 2022, respectively. They showed an overall accuracy (OA) higher than 90% for each period. The producer accuracy (PA) and user accuracy (UA) both ranged between 70% and

100%. These results indicate that the discrimination of all land cover was accurate. The analysis of disagreement between the land cover map and reference land cover showed that the allocation disagreement (AD) was smaller than the quantity disagreement (QD). The AD/QD ratio was 0.173, 0.747, 1.243 and 0.379 for 1990–1998, 1998–2008, 2008–2015 and 2015–2022, respectively. A low AD/QD ratio, as in this case, indicates a uniform distribution of misclassified pixels across the entire map [58]. All area estimates were significant, with no margin of error [57].

However, visual analysis of the land cover maps (Figure 3) indicated that miombo woodland experienced cover loss, while the grassland and wooded savannah experienced an increase in cover within the landscape. The regressive dynamics of the miombo woodland were high in the northeastern and northwestern LCPB. Water was excluded from the following analyses owing to its relative stability and low proportion in the landscape.
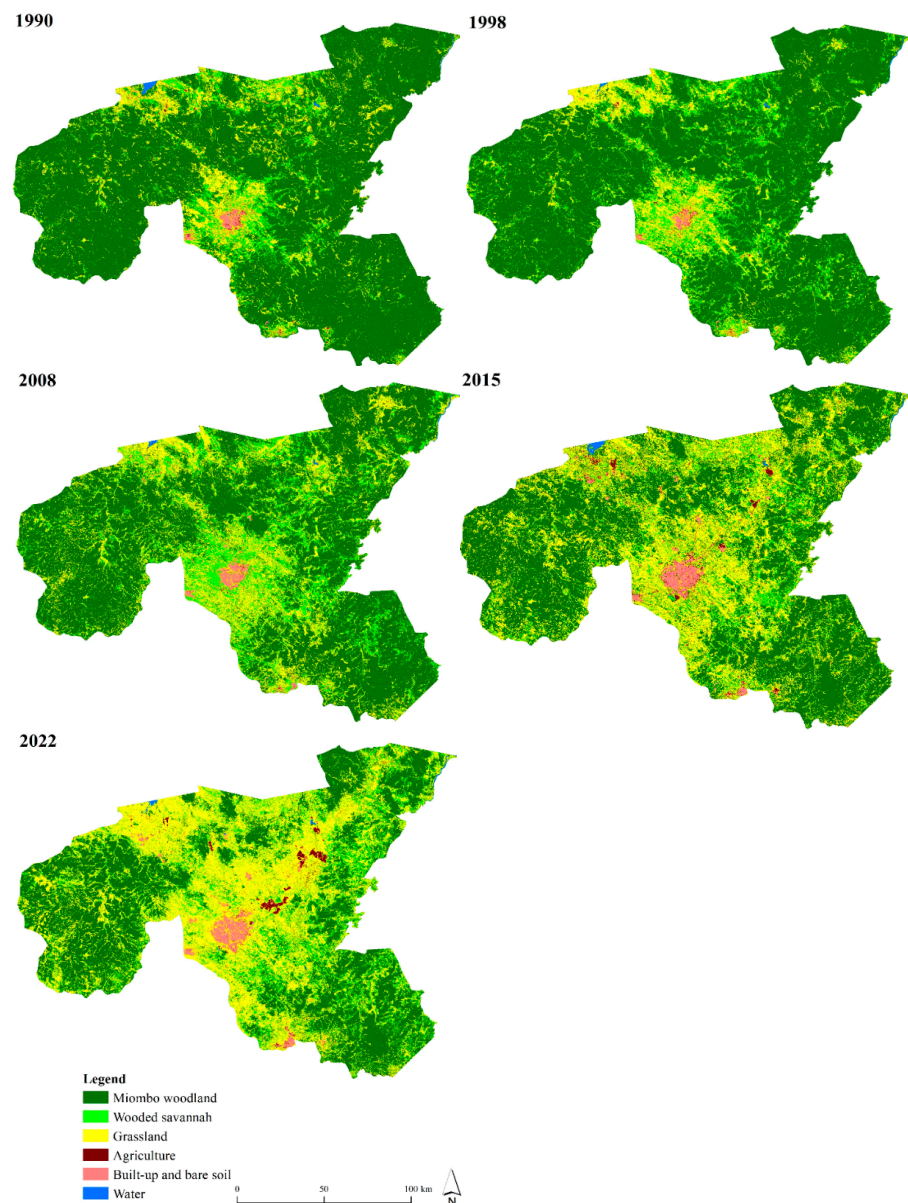
Figure 3. Land cover maps of the LCPB in 1990, 1998, 2008, 2015 and 2022 based on the supervised classification of the Landsat images using the random forest classifier. A decrease in the cover of the miombo woodland and an increase in wooded savannah, grassland, agriculture and built-up and bare soil were recorded.

Table 2. Accuracy assessment and area estimate for the land cover and land cover change map from 1990 to 1998 based on the Landsat image supervised classification using the random forest classifier. The values show that the classifications produced are statistically accurate. MW is miombo woodland; WS is wooded savannah; G is grassland; A is agriculture; BBS is built-up and bare soil, W is water; UA is user's accuracy; PA is producer accuracy; SE is standard error; OA is overall accuracy; CI is confidence interval; QD is quantity disagreement; AD is allocation disagreement.

| Map Class	Reference Class													
	M Stable	WS Stable	G Stable	A Stable	BBS Stable	W Stable	MW Loss	WS Gain	G Loss	A Gain	BBS Loss	Total	UA	UA SE
M stable	0.747	0.000	0.000	0.000	0.000	0.000	0.000	0.000	0.000	0.000	0.000	0.747	1.000	0.000
WS stable	0.000	0.036	0.000	0.000	0.000	0.000	0.000	0.000	0.000	0.000	0.000	0.036	1.000	0.000
G stable	0.000	0.000	0.062	0.000	0.000	0.000	0.000	0.000	0.000	0.000	0.000	0.062	1.000	0.000
A stable	0.000	0.000	0.000	0.000	0.000	0.000	0.000	0.000	0.000	0.000	0.000	0.000	0.811	0.035
BBS stable	0.000	0.000	0.000	0.000	0.003	0.000	0.000	0.000	0.000	0.000	0.000	0.003	1.000	0.000
W stable	0.000	0.000	0.000	0.000	0.000	0.001	0.000	0.000	0.000	0.000	0.000	0.001	1.000	0.000
MW loss	0.019	0.000	0.000	0.000	0.000	0.000	0.084	0.000	0.000	0.000	0.000	0.102	0.819	0.024
WS gain	0.000	0.004	0.000	0.000	0.000	0.000	0.004	0.030	0.000	0.000	0.000	0.038	0.808	0.026
G loss	0.000	0.000	0.000	0.000	0.000	0.000	0.000	0.000	0.001	0.000	0.000	0.001	0.707	0.038
A gain	0.000	0.000	0.000	0.000	0.000	0.000	0.000	0.000	0.000	0.002	0.000	0.002	1.000	0.000
BBS loss	0.000	0.000	0.000	0.000	0.000	0.000	0.000	0.000	0.000	0.000	0.007	0.007	1.000	0.000
Total	0.765	0.040	0.062	0.000	0.003	0.001	0.087	0.030	0.001	0.002	0.007	1.000		
PA	0.976	0.911	1.000	1.000	1.000	1.000	0.958	0.994	1.000	0.889	1.000			
PA SE	0.008	0.020	0.000	0.000	0.000	0.000	0.012	0.005	0.000	0.032	0.000			
OA	0.974													
OA SE	0.002													
QD	0.022													
AD	0.004													
AD/QD ratio	0.173													
Stratified estimators of area ± CI [% of total map area]														
Area (km^2)	18,970.62	982.455	1539.013	8.199	81.382	24.544	2168.283	755.742	19.215	48.511	167.367			
95% CI	0.481	0.141	0.000	0.003	0.000	0.000	0.502	0.190	0.008	0.007	0.000			

Table 3. Accuracy assessment and area estimate for the land cover and land cover change map from 1998 to 2008 based on the Landsat image supervised classification using the random forest classifier. The values show that the classifications produced are statistically accurate. MW is miombo woodland; WS is wooded savannah; G is grassland; A is agriculture; BBS is built-up and bare soil, W is water; UA is user's accuracy; PA is producer accuracy; SE is standard error; OA is overall accuracy; CI is confidence interval; QD is quantity disagreement; AD is allocation disagreement.

| Map Class | Reference Class | | | | | | | | | | | Total | UA | UA SE |
	MW Stable	WS Stable	G Stable	A Stable	BSS Stable	W Stable	MW Loss	WS Gain	G Gain	A Loss	BBS Gain			
MW stable	0.602	0.000	0.000	0.000	0.000	0.000	0.000	0.000	0.000	0.000	0.000	0.602	1.000	0.000
WS stable	0.000	0.044	0.000	0.000	0.000	0.000	0.000	0.000	0.004	0.000	0.000	0.048	0.921	0.018
G stable	0.000	0.000	0.072	0.000	0.000	0.000	0.000	0.000	0.000	0.000	0.000	0.072	1.000	0.000
A stable	0.000	0.000	0.000	0.000	0.000	0.000	0.000	0.000	0.000	0.000	0.000	0.000	1.000	0.000
BSS stable	0.000	0.000	0.000	0.000	0.003	0.000	0.000	0.000	0.000	0.000	0.000	0.003	1.000	0.000
W stable	0.000	0.000	0.000	0.000	0.000	0.001	0.000	0.000	0.000	0.000	0.000	0.001	1.000	0.000
MW loss	0.000	0.000	0.000	0.000	0.000	0.000	0.153	0.000	0.000	0.000	0.001	0.165	0.925	0.016
WS gain	0.000	0.000	0.000	0.000	0.000	0.000	0.013	0.031	0.000	0.000	0.000	0.044	0.711	0.037
G gain	0.000	0.000	0.000	0.000	0.000	0.000	0.016	0.000	0.040	0.000	0.000	0.056	0.714	0.038
A loss	0.000	0.000	0.000	0.000	0.000	0.000	0.000	0.000	0.000	0.002	0.000	0.002	1.000	0.000
BBS gain	0.000	0.000	0.000	0.000	0.001	0.000	0.000	0.000	0.000	0.001	0.005	0.006	0.778	0.037
Total	0.602	0.044	0.072	0.000	0.004	0.001	0.181	0.031	0.044	0.003	0.006	1.000		
PA	1.000	1.000	1.000	1.000	0.806	1.000	0.842	1.000	0.913	0.774	0.801			
PA SE	0.000	0.000	0.000	0.000	0.040	0.000	0.022	0.000	0.024	0.042	0.036			
OA	0.954													
OA SE	0.002													
QD	0.023													
AD	0.017													
AD/QD ratio	0.747													
Stratified estimators of area ± CI [% of total map area]														
Area (km^2)	15,691.887	1151.507	1865.410	4.968	108.873	24.287	5158.630	608.737	910.833	69.982	161.420			
95% CI	0.000	0.174	0.000	0.000	0.037	0.000	0.743	0.320	0.456	0.033	0.177			

Table 4. Accuracy assessment and area estimate for the land cover and land cover change map from 2008 to 2015 based on the Landsat image supervised classification using the random forest classifier. The values show that the classifications produced are statistically accurate. MW is miombo woodland; WS is wooded savannah; G is grassland; A is agriculture; BBS is built-up and bare soil, W is water; UA is user's accuracy; PA is producer accuracy; SE is standard error; OA is overall accuracy; CI is confidence interval; QD is quantity disagreement; AD is allocation disagreement.

Map Class	Reference Class													
	M Stable	WS Stable	G Stable	A Stable	BBS Stable	W Stable	MW Loss	WS Loss	G Gain	A Gain	BBS Gain	Total	UA	UA SE
M stable	0.563	0.000	0.000	0.000	0.000	0.000	0.000	0.000	0.000	0.000	0.000	0.563	1.000	0.000
WS stable	0.000	0.038	0.000	0.000	0.000	0.000	0.000	0.000	0.000	0.000	0.000	0.038	1.000	0.000
G stable	0.000	0.000	0.157	0.000	0.000	0.000	0.000	0.000	0.000	0.000	0.000	0.157	1.000	0.000
A stable	0.000	0.000	0.000	0.000	0.000	0.000	0.000	0.000	0.000	0.000	0.000	0.000	1.000	0.000
BBS stable	0.000	0.000	0.000	0.000	0.009	0.000	0.000	0.000	0.000	0.000	0.000	0.009	1.000	0.000
W stable	0.000	0.000	0.000	0.000	0.000	0.001	0.000	0.000	0.000	0.000	0.000	0.001	1.000	0.000
MW loss	0.000	0.005	0.000	0.000	0.000	0.000	0.037	0.000	0.009	0.000	0.000	0.050	0.732	0.034
WS loss	0.000	0.000	0.000	0.000	0.000	0.000	0.000	0.000	0.000	0.000	0.000	0.000	0.724	0.041
G gain	0.000	0.000	0.000	0.000	0.000	0.000	0.006	0.000	0.146	0.000	0.000	0.152	0.959	0.013
A gain	0.000	0.000	0.000	0.000	0.000	0.000	0.000	0.000	0.000	0.015	0.000	0.015	0.990	0.010
BBS gain	0.000	0.000	0.000	0.000	0.002	0.000	0.000	0.000	0.000	0.002	0.010	0.013	0.770	0.038
Total	0.563	0.043	0.157	0.001	0.010	0.001	0.043	0.000	0.155	0.017	0.010	1.000		
PA	1.000	0.888	1.000	0.720	0.854	1.000	0.854	1.000	0.944	0.908	1.000			
PA SE	0.000	0.023	0.000	0.045	0.035	0.000	0.027	0.000	0.015	0.029	0.001			
OA	0.976													
OA SE	0.002													
QD	0.010													
AD	0.013													
AD/QD ratio	1.243													
Stratified estimators of area ± CI [% of total map area]														
Area (km^2)	12,238.857	928.722	3406.855	12.216	226.836	28.256	935.510	0.362	3365.861	361.594	221.996			
95% CI	0.000	0.223	0.000	0.031	0.075	0.000	0.509	0.000	0.478	0.081	0.099			

Table 5. Accuracy assessment and area estimate for the land cover and land cover change map from 2015 to 2022 based on the Landsat image supervised classification using the random forest classifier. The values show that the classifications produced are statistically accurate. MW is miombo woodland; WS is wooded savannah; G is grassland; A is agriculture; BBS is built-up and bare soil, W is water; UA is user's accuracy; PA is producer accuracy; SE is standard error; OA is overall accuracy; CI is confidence interval; QD is quantity disagreement; AD is allocation disagreement.

| Map Class | Reference Class | | | | | | | | | | | | | |
	MW Stable	WS Stable	G Stable	A Stable	BSS Stable	W Stable	MW Loss	WS Gain	G Gain	A Gain	BBS Loss	Total	UA	UA SE
MW stable	0.363	0.000	0.000	0.000	0.000	0.000	0.000	0.000	0.000	0.000	0.000	0.363	1.000	0.000
WS stable	0.000	0.028	0.000	0.000	0.000	0.000	0.000	0.004	0.000	0.000	0.000	0.032	0.878	0.023
G stable	0.000	0.000	0.221	0.000	0.000	0.000	0.000	0.000	0.000	0.000	0.000	0.221	1.000	0.000
A stable	0.000	0.000	0.000	0.002	0.000	0.000	0.000	0.000	0.000	0.000	0.000	0.002	1.000	0.000
BSS stable	0.000	0.000	0.000	0.000	0.011	0.000	0.000	0.000	0.000	0.000	0.000	0.012	0.960	0.020
W stable	0.000	0.000	0.000	0.000	0.000	0.001	0.000	0.000	0.000	0.000	0.000	0.001	1.000	0.000
MW loss	0.015	0.000	0.006	0.000	0.000	0.000	0.180	0.000	0.000	0.002	0.000	0.203	0.885	0.019
WS gain	0.000	0.000	0.000	0.000	0.000	0.000	0.005	0.067	0.000	0.000	0.001	0.072	0.921	0.018
G gain	0.000	0.000	0.005	0.000	0.000	0.000	0.000	0.000	0.068	0.000	0.001	0.074	0.922	0.019
A gain	0.000	0.000	0.001	0.000	0.000	0.000	0.000	0.000	0.000	0.007	0.000	0.008	0.896	0.030
BBS loss	0.000	0.000	0.000	0.000	0.002	0.000	0.000	0.000	0.000	0.000	0.009	0.010	0.853	0.034
Total	0.379	0.028	0.233	0.002	0.013	0.001	0.185	0.071	0.068	0.009	0.012	0.999	0.900	0.030
PA	0.960	1.000	0.950	1.000	0.879	1.000	0.974	0.945	1.000	0.753	0.777			
PA SE	0.010	0.000	0.014	0.000	0.033	0.000	0.010	0.016	0.000	0.042	0.040			
OA	0.958													
OA SE	0.002													
QD	0.030													
AD	0.011													
AD/QD ratio	0.379													
Stratified estimators of area ± CI [% of total map area]														
Area (km²)	9577.292	707.382	5883.230	56.204	321.405	34.547	4667.587	1783.756	1720.688	232.245	291.278	19.967		
95% CI	0.638	0.143	0.483	0.000	0.083	0.000	0.813	0.299	0.272	0.259	0.187	0.005		

3.2. Landscape Composition Dynamics in the LCPB

The proportion of miombo woodland decreased by half from 77.98% in 1990 to 40.01% in 2022. During the same period, the wooded savannah doubled from 7.84% in 1990 to 15.62% in 2022. The proportion of grassland almost tripled from 12.99% in 1990 to 40.05% in 2022, and it became the new dominant land cover. Agriculture increased 12-fold from 1990 to 2022, even though its large patches appeared in the landscape only after 2008, and built and bare soil doubled during the same period (Table 6). The annual deforestation rate from 1990 to 2022 was –1.51%, resulting in a loss of 405.26 km^2 of miombo woodland per year.

Table 6. Transition matrices illustrating the percentage of land cover change between 1990 and 1998, 1998 and 2008, 2008 and 2015 and 2015 and 2022 based on the assisted classification of Landsat images using the random forest classifier. Values in bold indicate the proportion of land cover that remained unchanged, and 1% corresponds to 266 km^2. The totals do not add up to 100% as water was excluded from the analyses. Miombo woodland was the most disturbed land cover that was converted to other land covers.

1990–1998	Miombo Woodland	Wooded Savannah	Grassland	Agriculture	Built-Up and Bare Soil	Total
Miombo woodland	**68.52**	5.68	3.66	0.02	0.01	77.89
Wooded Savannah	1.46	**3.31**	3.00	0.02	0.05	7.84
Grassland	4.02	3.16	**5.64**	0.07	0.10	12.99
Agriculture	0.00	0.01	0.11	**0.03**	0.04	0.19
Built-up and Bare soil	0.00	0.13	0.38	0.04	**0.32**	0.86
Total	74.00	12.29	12.78	0.19	0.52	99.77
Stability index	4.61	0.25	0.39	0.10	0.43	

1998–2008	Miombo woodland	Wooded Savannah	Grassland	Agriculture	Built-up and Bare soil	Total
Miombo woodland	**58.52**	5.59	9.84	0.01	0.08	74.04
Wooded Savannah	2.41	**4.67**	5.10	0.02	0.13	12.34
Grassland	1.30	4.11	**6.91**	0.05	0.41	12.78
Agriculture	0.00	0.06	0.05	**0.02**	0.06	0.20
Built-up and Bare soil	0.00	0.07	0.10	0.01	**0.33**	0.52
Total	62.24	14.50	22.00	0.11	1.01	99.87
Stability index	3.04	0.27	0.33	0.08	0.38	

2008–2015	Miombo woodland	Wooded Savannah	Grassland	Agriculture	Built-up and Bare soil	Total
Miombo woodland	**45.82**	3.95	12.13	0.22	0.10	62.21
Wooded Savannah	2.51	**2.98**	8.07	0.44	0.51	14.51
Grassland	5.23	3.43	**12.40**	0.51	0.39	21.95
Agriculture	0.00	0.00	0.04	**0.03**	0.04	0.11
Built-up and Bare soil	0.00	0.03	0.11	0.12	**0.73**	0.99
Total	53.6	10.4	32.8	1.3	1.8	99.79
Stability index	1.90	0.16	0.41	0.09	0.56	

2015–2022	Miombo woodland	Wooded Savannah	Grassland	Agriculture	Built-up and Bare soil	Total
Miombo woodland	**33.70**	6.47	11.64	1.77	0.00	53.6
Wooded Savannah	1.41	**2.75**	6.01	0.12	0.09	10.4
Grassland	4.87	6.32	**21.06**	0.29	0.26	32.8
Agriculture	0.01	0.08	0.87	**0.21**	0.14	1.3
Built-up and Bare soil	0.01	0.01	0.48	0.11	**1.15**	1.8
Total	40.01	15.62	40.05	2.50	1.65	99.8
Stability index	1.29	0.13	0.69	0.06	1.05	

The dynamics of miombo woodland were supported by a transfer of its acreage to wooded savannah (5.68% from 1990 to 1998 and 6.47% from 2015 to 2022). This dynamic was also supported by a transfer of its acreage to grassland (3.66%, 9.84%, 12.13% and 11.64% for 1990–1998, 1998–2008, 2008–2015 and 2015–2022, respectively). However, the expansion of wooded savannah was supported by the transfer of acreages from miombo woodland (21.68%), recovery from grassland (17.01%), agriculture (0.15%) and built-up and bare soil (0.24%). The increase in the grassland acreage was mainly supported by a high transfer of acreage from miombo woodland (37.26%) and wooded savannah (22.18%) from 2008 to 2015. Agriculture has experienced significant growth, especially from 2008 to 2014 and from 2015 to 2022, supported by a transfer from miombo woodland (2.03%), wooded savannah (0.60%), grassland (0.92%) and built-up and bare soil (0.28%). However, built-up and bare soil area increased in the LCPB landscape because of the high transfer of acreage from miombo woodland (0.19%), wooded savannah (0.78), grassland (1.15%) and agriculture (0.28%) between 2008 and 2015 (Table 6).

The miombo woodland showed low dynamics from 1990 to 1998 and from 1998 to 2008, as evidenced by the high stability index values during these periods of 4.6 and 3.04, respectively. In contrast, the periods of 2008–2015 and 2015–2022 had low values of this index of 1.9 and 1.29, respectively, indicating high dynamics. However, wooded savannah, grassland, agriculture and built-up and bare soil all showed high dynamics during all periods, as reflected by the stability index values below (Table 6). However, the analysis of landscape diversity showed that Simpson's diversity index almost doubled from 0.37 in 1990 to 0.64 in 2022. This revealed a decreasing level of homogeneity of the LCPB landscape with time, manifested by increased patch diversity. The increased diversity was accompanied by almost a doubling in the evenness between patches in the landscape, as shown by the increased Simpson's evenness index (SIEI) from 0.44 in 1990 to 0.77 in 2022 (Table 7).

Table 7. Simpson's diversity index (SIDI) and Simpson's evenness index (SIEI) of the LCPB in 1990, 1998, 2008, 2015 and 2022.

Year	SIDI	SIEI
1990	0.37	0.44
1998	0.42	0.50
2008	0.54	0.65
2015	0.59	0.71
2022	0.64	0.77

3.3. Structural Dynamics in the LCPB

Our analysis of the landscape structural dynamics of the LCPB showed that the 1990–1998 period was characterised by the attrition of miombo woodlands and grasslands as the dominant spatial transformation process (Table 8). However, during this period, wooded savannah and agriculture underwent creation process. Additionally, built-up and bare soil underwent aggregation. The period of 1998–2008 was characterised by a dissection of the miombo woodland area (*t*-value 0.83 > 0.75). Wooded savannah, grasslands and built-up and bare soil underwent a creation process. In contrast, the agriculture class underwent attrition. During the 2008–2015 period, miombo was characterized by dissection (*t*-value of 0.86 > 0.75). The wooded savannah showed fragmentation with a *t*-value of 0.71 < 0.75. Grassland, agriculture and built-up and bare soil expanded through creation. Finally, during the 2015–2022 period, there was an attrition of miombo woodland. Wooded savannah, agriculture and built-up and bare soil underwent creation. During the same period, grassland underwent aggregation (Table 8).

Table 8. Summary of landscape metric characteristic of the LCPB dynamics for 1990, 1998, 2008, 2015 and 2022 based on the supervised classification of Landsat images using the random forest classifier. Here, *n* is the number of patches, *a* is the class area (km^2), *LPI* is the largest patch index (%), and *FD* is the fractal dimension. The miombo woodland underwent fragmentation, dissection and suppression as evidenced by the decreased or increased number of patches, and its decrease in area, largest patch index and fractal dimension.

Index	Miombo Woodland	Wooded Savannah	Grassland	Agriculture	Built-Up and Bare Soil
			1990		
n	175,136	323,591	404,735	12,514	66,436
a	20,722.88	2092.47	3473.78	51,06	231.95
LPI	74.39	0.35	1.26	0.004	0.30
FD	1.45	1.50	1.47	1.42	1.51
			1998		
n	157,750	546,619	300,589	23,657	21,075
a	19,697.76	3156.87	3421.39	53.12	246
LPI	70.55	0.30	2.73	0.01	0.20
FD	1.44	1.52	1.44	1.51	1.45
			2008		
n	252,518	586,753	619,337	20,200	31,609
a	16,520.891	3817.7	5935.24	30.92	267.87
LPI	54.14	0.71	2.99	0.001	0.44
FD	1.45	1.50	1.47	1.51	1.46
			2015		
n	533,592	815,645	937,317	128,788	48,931
a	14,249.0919	2712.91	8763.54	345.79	475.12
LPI	20.56	0.18	11.72	0.04	0.86
FD	1.50	1.56	1.53	1.48	1.46
			2022		
n	240,244	940,122	504,829	349,199	54,711
a	10,643.61	4154.48	10,664.64	664.58	494.01
LPI	9.20	0.30	27.19	0.12	0.79
FD	1.42	1.55	1.48	1.40	1.43

The area of the largest patch of miombo woodland decreased from 74.39% in 1990 to 9.20% in 2022, indicating a fragmentation of miombo woodland patches. In contrast, the largest patch index (LPI) for the grassland increased from 2.13% in 1990 to 27.19% in 2022. Wooded savannah, agriculture and built-up and bare soil all had low LPI values (less than 1) throughout the period. The fractal dimension value slightly decreased for the miombo woodland, from 1.45 to 1.42 between 1990 and 2022, indicating that some miombo woodland patches have a regular shape, a characteristic of anthropisation. Conversely, the fractal dimension value increased for the savannah, from 1.50 in 1990 to 1.55 in 2022, indicating that some patches have a more regular shape. The fractal dimension value for the grassland increased from 1.47 in 1990 to 1.48 in 2022, indicating that patches almost retained the same shape. Agriculture had the lowest fractal dimension values, from 1.42 in 1990 to 1.40 in 2022, owing to the regular shape that characterises its patches. Finally, built-up and bare soil showed a decrease in its fractal dimension value, from 1.51 in 1990 to 1.43 in 2022, showing a change in the shape of its patches over time (Table 8).

4. Discussion

4.1. Dynamics of the Anthropisation of the Miombo Forest in the LCPB

The classifications of Landsat images in this study showed OA values greater than 90%. In fact, overall accuracy values above 80% are highly accurate, indicating a high

level of agreement between estimated classes and reference classes [46,49]. Moreover, our results showed that the AD and QD values are close, with a correspondingly low allocation disagreement to quantity disagreement (AD/QD) ratio, indicating substantial overall disagreement [67]. Our values are lower than those found in Ref. [59].

Landscape analysis of the LCPB has shown remarkable dynamics, as evident by the regression of miombo woodland (natural and dominant cover), where its area was divided nearly in half between 1990 and 2022. The resulting general trends in LCPB anthropisation confirm the conclusions of numerous studies in the Katanga region, a historic mining area [20,22,23,32,35,68]. This would be justified by the use of the same approach despite the difference in analysis tools. The anthropogenic pressure on the miombo woodland is motivated by the demographic growth of Lubumbashi [28,68]. Indeed, the social situation in the region, which includes rapid population growth, uneven allocation of resources and poverty, has played a part in the depletion of miombo woodland [69]. The local culture has also played a significant role as well. For centuries, local communities have engaged in shifting agriculture and logging for subsistence. This practice, coupled with rapid population growth, has resulted in deforestation [70]. Recently, intensive and extensive agricultural activities have increased around the city of Lubumbashi, threatening the existence of the miombo woodland that once dominated the Katangese landscape [27]. One study [24] confirmed this trend around the urban areas of Southern Katanga. In the Zambezian region, Ref. [71] showed significant changes in land cover/use between 2000 and 2010, with an increase in agricultural area and a decrease in miombo woodlands in Zimbabwe.

Political factors have also played a major role in the regression of miombo woodland cover in Katanga. Political instability, corruption, and weak enforcement of legal texts have been associated with environmental degradation. Indeed, the forestry code drawn up in 2002, inspired (too much) by the Cameroonian model and its equatorial forests, is far less adapted to the reality of the miombo woodland. This forestry code has not provided a forest management plan. People no longer refer to it because of the many cases of impunity. Provincial tax documents supplement this single legal document, which explains the predominant tax collection role played by the provincial services, whereas the role of supervising the actors involved in the exploitation of forest resources is weak [40].

Deforestation of the miombo woodland has led to an increase in wooded savannah and grassland, leading to negative spatial conversion dynamics for the natural ecosystem in the LCPB. This regression of miombo woodland cover is a direct consequence of wood cutting for charcoal production. Indeed, the galloping growth of Lubumbashi's population, coupled with the insufficient production and distribution of electrical energy, leads to the dependence of almost all urban households on miombo forest for charcoal [72]. These results confirm the conclusions of Ref. [29], which states that charcoal production is one of the main causes of forest fragmentation and degradation in Katanga. The rapid forest regression in the Lubumbashi region is motivated by the ease of accessibility to resources around Lubumbashi. Access to the forest is negotiated with customary chiefs in exchange for certain tributes and regular gifts for locals and approximately USD 20 for foreigners [73]. In this region, large forest patches are cut without any selection of plant species or stem diameter, while professional charcoal producers acquire large areas from traditional authorities around the city of Lubumbashi for exploitation. In the Zambezi ecoregion, Ref. [74] reported that clear-cutting of miombo forest, particularly for charcoal production, has led to forest degradation in Zambia, while also highlighting the low rate of forest regeneration in this region, endangering the sustainability of charcoal for the population. Ref. [75] also confirmed forest degradation associated with charcoal production in the Tete province in Mozambique.

The regression of miombo woodland cover has been significant in the northwestern and northeastern parts of the LCPB, due to the creation and rehabilitation of economic roads that have facilitated access to the forest, leading to its fragmentation [76,77]. The significant anthropogenic pressure on the LCPB has been confirmed by changes in the SIDI

and SIEH indices since less disturbed landscapes are characterized by low values of these indices [78].

The analysis of landscape dynamics in the miombo woodland within the LCBP revealed that the dominant spatial transformation processes are dissection and attrition, which are characteristic of natural land-cover-type dynamics [65]. Indeed, dissection in the miombo woodland surrounding Lubumbashi is primarily the result of the construction or rehabilitation of agricultural roads funded by mining companies for territorial entities, according to Ref. [79]. Consecutively, the attrition of persistent miombo woodland patches is a consequence of continuous deforestation that results in savannah, grassland and agriculture. These findings confirm the conclusions of Refs. [22,23] regarding the Lubumbashi Plain and the Katanga Copperbelt. Wooded savannah, grassland, agriculture and built-up and bare soil primarily underwent creation as the main transformation process, which is characteristic of anthropogenic land-cover-type dynamics [65]. The creation of wooded savannah patches in the LCPB landscape is caused by openings, which allow for the development of herbaceous plants that are primarily heliophilic. Ref. [27] stated that, in general, savannahs increase in a region owing to human activities. Our findings confirm the results of Ref. [35], that woody savannah patches increased on the Lubumbashi Plain in the LCBP. The increase in agricultural patches resulted from a new policy from the local government to reduce maize importation by granting improved seeds and inputs since 2006 to agricultural households. The creation of built-up and bare soil patches is attributed to the spatial expansion of built-up soil within Lubumbashi [67] upon the replacement of the dominant wooded savannah and grassland with peri-urban areas. This trend also confirms the conclusion by Ref. [38] in their study of the Lufira Biosphere Reserve in the LCBP, despite the difference in spatial scales between the two studies.

In the LCBP, the deforestation rate between 1990 and 2022 was higher than the national average, which was estimated to be between −0.2% and −0.3% [20,80]. This can be justified by the difference in the analysis scale. Furthermore, the extent of miombo woodland regression was weaker between 1990 and 1998 due to social and economic crises. Indeed, since 1990, Katanga has experienced a period of political instability that has led to the failure of state institutions and public companies to carry out their regal responsibilities. Although current Congolese law protects the forests against any form of degradation or destruction since the promulgation of forest code in 2002, the provincial services, which are made up of more administrative than technical staff, are unable to visibly apply these legal provisions [45]. In addition, the period between 1998 and 2008 resulting from the liberalisation of mining activities led to an improvement in the socioeconomic conditions of the urban population [28]. However, as a result, there was strong pressure on miombo woodland for charcoal production and its conversion into grassland [29,35]. Also, peasants shifted away from agriculture towards artisanal mining activities, consequently destroying forest resources [81]. However, during the period following the global economic crisis of 2008, many development projects were suspended or cancelled, leading to a decrease in investments within the Katanga forestry sector, particularly in rural areas. As investment decreased, environmental regulations were also weakened, resulting in an increase in illegal exploitation of forest resources [34]. Finally, the intensification of miombo regression between 2015 and 2022 was a result of the dismantling of the former Katanga Province and the local government's agricultural policy. Indeed, through this policy, the government aims to ensure that its population is self-sufficient in maize by granting agricultural inputs to farmers who have consequently extended the acreage of their fields to the detriment of forest patches. This period was also characterised by conversions of forests to wooded savannah, which was a consequence of the growing demand for charcoal in the region [29]. Between 2015 and 2022, the production of wood fuel became one of the most alarming anthropogenic causes of the deforestation of miombo woodland, given that the national electricity society favours the new mining companies installed since 2015 to the detriment of households. Urban growth and the lack of electricity supply are increasing the demand for wood fuel and timber [29].

The negative spatial dynamics of miombo in the LCBP were accompanied by low densification and regeneration. This may have been caused by recurring vegetation fires in the region and the conversion of areas into agricultural land that were exploited for charcoal production [19,39]. These justify the decrease in the stability of miombo land cover, which is supported by the three-fold decrease in its stability index value, a trend also confirmed previously in Ref. [34] in Kasenga territory to the east of the LCPB.

The analysis of the LCPB landscape also showed fragmentation of the miombo woodland, as demonstrated by the eight-fold decrease in the LPI. However, Ref. [25] indicated a two-fold decrease in the LPI in Lubumbashi. This difference could be due to the difference in spatial and temporal scales. The low values of this index obtained for wooded savannah, grassland, agriculture and built-up and bare soil illustrate their high degree of anthropisation. The obtained values of the fractal dimension show the impact of human activities on the landscape structure, which is reflected in the more homogeneous and regular shapes of landscape elements [65].

Our landscape analysis results within the LBPC confirm the perceptions of local communities who note a decline in woody cover in the region, whether in the peri-urban area [82] or in the rural area of the city of Lubumbashi [40,83]. However, in a country where one person lives on an average of less than USD 1.25 per day, and where the forestry code suffers from lack of enforcement, forest resources provide a source of food, medicine, construction materials or even income when sold in rural or urban markets [38,73].

4.2. Implications for the Management of the LCPB

This study clarified the decline in the miombo woodland (loss in area) in the LCPB. This decrease in miombo highlights the threat to the provision of ecosystem services. The consequent distance of the city from the forest means that charcoal will be produced further away [44], which will impact the price of this main energy source for the city. Miombo deforestation will lead to a significant decrease in products, such as mushrooms, caterpillars, honey and certain edible fruits, which are some of the natural resources that the Congolese population uses to improve its income and food safety [84,85].

In a developing nation with high rates of unemployment, where more than 90% of the population relies on charcoal as a source of sustenance [29], forest degradation may have challenging socioeconomic ramifications. Charcoal production in Lubumbashi, for instance, yields an estimated annual total added value of approximately USD 50 million [86], making it a crucial source of livelihood for charcoal-producing and -selling households. Additionally, miombo forest regression could instigate land use conflicts among diverse communities. On the other hand, certain forest products, such as timber and non-timber forest products, are imported from Zambia, leading to a political dependence of the country on its neighbor.

Wood energy producers include farmers, who derive income from charcoal to supplement their agricultural production (maize, manioc, sweet potatoes and groundnuts) and professional producers whose main aim is to produce charcoal. In addition to species that produce good-quality wood fuel, in the context of high competition for resource access, charcoal producers are now choosing less sought-after species, even within patches of sacred forest. As a result, the distances involved in acquiring wood for charcoal production are increasing, leading to higher harvesting costs.

As degraded ecosystems that materialise from the savannah are expanding within the LCPB, a policy towards expanding community forests is required. This policy should have a management plan that defines and maps the conservation areas of miombo. Ref. [87] also advised moving from open access forests to secure tenure and sustainable forest management in Zambia. The management plan for community forests must define the support for natural regeneration through reforestation and fire management. Examples of successful community forestry projects in Gambia, Tanzania and Brazil are described in Ref. [88]. Additionally, some miombo species were proposed in Ref. [89] for the reforestation of degraded ecosystems. However, as charcoal is ingrained in the local culture, scientific

research identifying miombo species with high calorific capacity and rapid regeneration for introduction into the reforestation program is needed in the short term. Moreover, exotic species should be avoided as they can contribute to the eradication of native species [90].

This policy should also be focused on agroforestry, which is an integrated natural resource management intervention that can address various environmental and social problems in Eastern and Southern Africa [91]. Ref. [92] demonstrated the important contributions of rotational woodlot systems in reducing forest degradation and offsetting CO_2 emissions through on-farm wood supply. However, the management policy should also consider different techniques, such as crop rotation and intercropping, which are effective practices for soil fertility management [93].

Within Lubumbashi, the use of improved cookstoves and public investment in hydro and solar power generation is crucial for reducing the pressure on the remnants of miombo woodland patches while meeting the energy needs of the urban population. Efforts should also be focused on their adoption by the population, as improved stoves are already widely used in the Sahelian region and in countries, such as Mali and Burkina Faso [94].

Finally, it is also important for political authorities to consider improving the living conditions of rural populations in order to prevent mass migration to urban areas.

5. Conclusions

In this study, we quantified the evolution of deforestation of miombo woodland in the LCPB using remote sensing combined with landscape ecology analysis tools. Our results confirm that miombo woodland acreage has decreased over time via the expansion of wooded savannah and grassland and transformation into agricultural land. This has resulted in the fragmentation and anthropisation of the landscape, with the largest patch of miombo and its complexity decreasing, as shown by increases in the SIDI and SIEI values. The analysis also identified five spatial transformation processes: attrition and dissection of miombo woodland; fragmentation and creation of wooded savannah; attrition, creation and aggregation of grassland; attrition and creation of cultivated land; and creation and aggregation of built-up and bare soil. Additionally, we found that the deforestation rate within the LCBP is higher than the national average. In this context, the regression of the miombo woodland forest increases the distance between Lubumbashi and charcoal production areas, which can have consequences in terms of availability and price.

To address the regression of miombo woodland in the LCPB, we should implement policies that multiply community forests and develop agroforestry, finance large-scale reforestation, promote the use of improved stoves and invest in hydroelectricity and solar energy. These are critical for reducing the pressure on the miombo woodland in the LCPB while meeting the energy needs of the urban population. In the future, it will be necessary to demonstrate the impact of deforestation on the local climate.

Author Contributions: H.K.M.: formal analysis and writing—original draft, D.-d.N.N.: writing—review, F.M.K. (Franco Mwamba Kalenda): writing—review, H.S.: writing—review, F.M.: writing—review, F.M.K. (François Munyemba Kankumbi): writing—review, J.-F.B.: writing—review, Y.U.S.: supervision and writing—original draft, J.B.: supervision and writing—original draft. All authors have read and agreed to the published version of the manuscript.

Data Availability Statement: The data presented in this study are available on request from the corresponding author.

Conflicts of Interest: The authors declare no conflict of interest.

References

1. Shackleton, C.M.; Shackleton, S.E.; Buiten, E.; Bird, N. The Importance of Dry Woodlands and Forests in Rural Livelihoods and Poverty Alleviation in South Africa. *For. Policy Econ.* **2007**, *9*, 558–577. [CrossRef]
2. HLPE. *Sustainable Forestry for Food Security and Nutrition*; A report by the high level panel of experts on food security and nutrition of the committee on World Food Security; HLPE: Rome, Italy, 2017.

3. Sunderland, T.; Powell, B.; Ickowitz, A.; Foli, S.; Pinedo-Vasquez, M.; Nasi, R.; Padoch, C. *Food Security and Nutrition*; Center for International Forestry Research (CIFOR): Bogor, Indonesia, 2013.

4. Foli, S.; Reed, J.; Clendenning, J.; Petrokofsky, G.; Padoch, C.; Sunderland, T. To What Extent Does the Presence of Forests and Trees Contribute to Food Production in Humid and Dry Forest Landscapes?: A Systematic Review Protocol. *Environ. Evid.* **2014**, *3*, 15. [CrossRef]

5. Reed, J.; van Vianen, J.; Foli, S.; Clendenning, J.; Yang, K.; MacDonald, M.; Petrokofsky, G.; Padoch, C.; Sunderland, T. Trees for Life: The Ecosystem Service Contribution of Trees to Food Production and Livelihoods in the Tropics. *For. Policy Econ.* **2017**, *84*, 62–71. [CrossRef]

6. Agariga, F.; Abugre, S.; Appiah, M. Spatio-Temporal Changes in Land Use and Forest Cover in the Asutifi North District of Ahafo Region of Ghana, (1986–2020). *Environ. Chall.* **2021**, *5*, 100209. [CrossRef]

7. Ter Steege, H.; Pitman, N.C.A.; Killeen, T.J.; Laurance, W.F.; Peres, C.A.; Guevara, J.E.; Salomão, R.P.; Castilho, C.V.; Amaral, I.L.; de Almeida Matos, F.D.; et al. Estimating the Global Conservation Status of More than 15,000 Amazonian Tree Species. *Sci. Adv.* **2015**, *1*, e1500936. [CrossRef] [PubMed]

8. Hansen, M.C.; Potapov, P.V.; Moore, R.; Hancher, M.; Turubanova, S.A.; Tyukavina, A.; Thau, D.; Stehman, S.V.; Goetz, S.J.; Loveland, T.R.; et al. High-Resolution Global Maps of 21st-Century Forest Cover Change. *Science* **2013**, *342*, 850–853. [CrossRef] [PubMed]

9. Barlow, J.; Lennox, G.D.; Ferreira, J.; Berenguer, E.; Lees, A.C.; Nally, R.M.; Thomson, J.R.; de Barros Ferraz, S.F.; Louzada, J.; Oliveira, V.H.F.; et al. Anthropogenic Disturbance in Tropical Forests Can Double Biodiversity Loss from Deforestation. *Nature* **2016**, *535*, 144–147. [CrossRef]

10. Sánchez, J.J.; Marcos-Martinez, R.; Srivastava, L.; Soonsawad, N. Valuing the Impacts of Forest Disturbances on Ecosystem Services: An Examination of Recreation and Climate Regulation Services in U.S. National Forests. *Trees For. People* **2021**, *5*, 100123. [CrossRef]

11. FAO. *Global Forest Resources Assessment 2020*; FAO: Rome, Italy, 2020; ISBN 978-92-5-132974-0.

12. Müller, C. *Brazil and the Amazon Rainforest: Deforestation, Biodiversity and Cooperation with the EU and International Forums*; In-depth analysis for the committee on the Environment, Public Health and Food Safety of the European Parliament; Policy Department for Economic, Scientific and Quality of Life Policies Directorate-General for Internal Policies: Luxembourg, 2020.

13. Sasaki, N.; Myint, Y.Y.; Venkatappa, M. Assessment of the Forest Carbon Balance Due to Deforestation and Plantation Forestry in Southeast Asia. In *Energy Sustainability and Climate Change in ASEAN*; Phoumin, H., Taghizadeh-Hesary, F., Kimura, F., Arima, J., Eds.; Sur l'économie, le Droit et les Institutions en Asie-Pacifique; Springer: Singapore, 2021; pp. 89–110. ISBN 9789811620003.

14. FAO. FAOSTAT Database. Available online: https://www.fao.org/faostat/en/#data/FO (accessed on 12 December 2022).

15. FAO. *Évaluation des Ressources Forestières Mondiales 2010*; UNFAO: Rome, Italy, 2010.

16. Tchatchou, B.; Sonwa, D.J.; Ifo, S.; Tiani, A.M. *Déforestation et Dégradation des Forêts Dans le Bassin du Congo: État Des Lieux, Causes Actuelles et Perspectives*; Center for International Forestry Research (CIFOR): Bogor, Indonesia, 2015; ISBN 978-602-1504-69-7.

17. Zhuravleva, I.; Turubanova, S.; Potapov, P.; Hansen, M.; Tyukavina, A.; Minnemeyer, S.; Laporte, N.; Goetz, S.; Verbelen, F.; Thies, C. Satellite-Based Primary Forest Degradation Assessment in the Democratic Republic of the Congo, 2000–2010. *Environ. Res. Lett.* **2013**, *8*, 024034. [CrossRef]

18. Megevand, C.; Mosnier, A.; Hourticq, J.; Sanders, K.; Doetinchem, N.; Streck, C. *Dynamiques de Deforestation Dans le Basin du Congo: Reconcilier la Croissance Economique et la Protection de la Foret*; The World Bank: Washington, DC, USA, 2013; ISBN 978-0-8213-9838-8.

19. Ministère de l'Environnement Conservation de la Nature et Tourisme. *Synthèse des Études sur les Causes de la Déforestation et de la Dégradation des Forêts en République Démocratique du Congo*, Version finale; 2012. Available online: https://www.forestcarbonpartnership.org/sites/fcp/files/2015/March/12-08-08%20PI%20Causes%20Etude%20qualitative%20causes%20DD%20PNUE.pdf (accessed on 24 September 2023).

20. Potapov, P.V.; Turubanova, S.A.; Hansen, M.C.; Adusei, B.; Broich, M.; Altstatt, A.; Mane, L.; Justice, C.O. Quantifying Forest Cover Loss in Democratic Republic of the Congo, 2000–2010, with Landsat ETM+ Data. *Remote Sens. Environ.* **2012**, *122*, 106–116. [CrossRef]

21. Meerts, P.; Hasson, M. *Arbres et Arbustes du Haut-Katanga*; Jardin Botanique de Meise: Meise, Belgium, 2017.

22. Cabala, K.S.; Useni, S.Y.; Kouagou, R.S.; Bogaert, J.; Munyemba, K.F. Dynamique Des Écosystémes Forestiers de I'Arc Cuprifére Katangais En République Démocratique Du Congo. I. Causes, Transformations Spatiales et Ampleur. *Tropicultura* **2017**, *35*, 192–202.

23. Cabala, K.S.; Useni, S.Y.; Munyemba, K.F.; Bogaert, J. Activités Anthropiques et Dynamique Spatiotemporelle de La Forêt Claire Dans La Plaine de Lubumbashi. In *Anthropisation des Paysages Katangais*; Bogaert, J., Colinet, G., Mahy, G., Eds.; Presses Universitaires de Liège: Liège, Belgique, 2018; pp. 253–266.

24. Khoji, M.H.; N'Tambwe, D.-D.; Malaisse, F.; Waselin, S.; Sambiéni, K.R.; Cabala, K.S.; Munyemba, K.F.; Bastin, J.-F.; Bogaert, J.; Useni, S.Y. Quantification and Simulation of Landscape Anthropization around the Mining Agglomerations of Southeastern Katanga (DR Congo) between 1979 and 2090. *Land* **2022**, *11*, 850. [CrossRef]

25. Useni, S.Y.; André, M.; Mahy, G.; Cabala, K.S.; Malaisse, F.; Munyemba, K.F.; Bogaert, J. Interprétation Paysagère Du Processus d'urbanisation à Lubumbashi: Dynamique de La Structure Spatiale et Suivi Des Indicateurs Écologiques Entre 2002 et 2008. In *Anthropisation des Paysages Katangais*; Bogaert, J., Colinet, G., Mahy, G., Eds.; Presses Universitaires de Liège: Liège, Belgique, 2018; pp. 281–296.

26.   Useni, S.Y.; Malaisse, F.; Cabala, K.S.; Kalumba, M.A.; Amisi, M.; Nkuku, K.C.; Bogaert, J.; Munyemba, K.F. Tree Diversity and Structure on Green Space of Urban and Peri-Urban Zones: The Case of Lubumbashi City in the Democratic Republic of Congo. *Urban For. Urban Green.* **2019**, *41*, 67–74. [CrossRef]

27.   Malaisse, F. *How to Live and Survive in Zambezian Open Forest (Miombo Ecoregion)*; Les Presses Agronomiques de Gembloux: Gembloux, Belgium, 2010; Volume 23, pp. 91–97.

28.   Nkuku, K.C.; Rémon, M. *Stratégies de Survie à Lubumbashi (RD Congo). Enquête Sur 14000 Ménages Urbains*; Mémoires lieux de savoir: Archive congolaise; Le Harmattan: Paris, France, 2006.

29.   Kabulu, D.J.-P.; Vranken, I.; Bastin, J.-F.; Malaisse, F.; Nyembwe, N.S.; Useni, S.Y.; Ngongo, L.M.; Bogaert, J. Approvisionnement En Charbon de Bois Des Ménages Lushois: Quantités, Alternatives et Conséquences. In *Anthropisation des Paysages Katangais*; Bogaert, J., Colinet, G., Mahy, G., Eds.; Presses Universitaires de Liège: Liège, Belgique, 2018; pp. 297–311.

30.   United Nations. *World Population Prospects*; UN DESA/POP/2022/TR/NO. 3; United Nations: Geneva, Switzerland, 2022.

31.   Crowley, M.A.; Cardille, J.A. Remote Sensing's Recent and Future Contributions to Landscape Ecology. *Curr. Landsc. Ecol. Rep.* **2020**, *5*, 45–57. [CrossRef]

32.   Barima, Y.S.S.; Kabulu, D.J.-P.; Ndayishimiye, J.; Bomolo, O.; Kumba, S.; Iyongo, L.; Bamba, I.; Toyi, M.; Kasongo, E.; Masharabu, T.; et al. Deforestation in Central and West Africa: Landcapes Dynamics, Anthropigenic Effects and Ecological Consequences. *Adv. Environ. Res.* **2011**, *7*, 95–120.

33.   Kabulu, D.J.; Bamba, I.; Munyemba, K.F.; Defourny, P.; Vancutsem, C.; Nyembwe, N.S.; Ngongo, L.M.; Bogaert, J. Analyse de La Structure Spatiale Des Forêts Au Katanga. *Ann. Fac. Sci. Agron.* **2008**, *1*, 12–18.

34.   Mpanda, M.M.; Khoji, M.H.; N'Tambwe, N.D.-D.; Sambiéni, K.R.; Malaisse, F.; Cabala, K.S.; Bogaert, J.; Useni, S.Y. Uncontrolled Exploitation of Pterocarpus Tinctorius Welw. and Associated Landscape Dynamics in the Kasenga Territory: Case of the Rural Area of Kasomeno (DR Congo). *Land* **2022**, *11*, 1541. [CrossRef]

35.   Munyemba, K.F.; Bogaert, J. Anthropisation et Dynamique Spatiotemporelle de l'occupation Du Sol Dans La Région de Lubumbashi Entre 1956 et 2009. *E Rev. UNILU* **2014**, *1*, 1–23.

36.   Useni, S.Y.; Cabala, K.S.; Halleux, J.M.; Bogaert, J.; Munyemba, K.F. Caractérisation de la croissance spatiale urbaine de la ville de Lubumbashi (Haut-Katanga, R.D. Congo) entre 1989 et 2014. *Tropicultura* **2018**, *36*, 99–108.

37.   Useni, S.Y.; Boisson, S.; Cabala, K.S.; Nkuku, K.C.; Malaisse, F.; Halleux, J.-M.; Bogaert, J.; Munyemba, K.F. Dynamique de l'occupation du sol autour des sites miniers le long du gradient urbain-rural de la ville de Lubumbashi, RD Congo. *Biotechnol. Agron. Soc. Environ.* **2020**, *24*, 14–27.

38.   Useni, S.Y.; Khoji, M.H.; Bogaert, J. Miombo Woodland, an Ecosystem at Risk of Disappearance in the Lufira Biosphere Reserve (Upper Katanga, DR Congo)? A 39-Years Analysis Based on Landsat Images. *Glob. Ecol. Conserv.* **2020**, *24*, e01333.

39.   Useni, S.Y.; Mpanda, M.M.; Malaisse, F.; Kazaba, K.P.; Bogaert, J. The Spatiotemporal Changing Dynamics of Miombo Deforestation and Illegal Human Activities for Forest Fire in Kundelungu National Park, Democratic Republic of the Congo. *Fire* **2023**, *6*, 174. [CrossRef]

40.   N'tambwe, N.D.-D.; Khoji, M.H.; Kasongo, B.W.N.; Sambiéni, K.R.; Malaisse, F.; Useni, S.Y.; Masengo, K.W.; Bogaert, J. Towards an Inclusive Approach to Forest Management: Highlight of the Perception and Participation of Local Communities in the Management of Miombo Woodlands around Lubumbashi (Haut-Katanga, D.R. Congo). *Forests* **2023**, *14*, 687. [CrossRef]

41.   Kottek, M.; Grieser, J.; Beck, C.; Rudolf, B.; Rubel, F. World Map of the Köppen-Geiger Climate Classification Updated. *Meteorol. Z.* **2006**, *15*, 259–263. [CrossRef]

42.   Malaisse, F. Phenology of Zambezian Wodland Area with Emphasis on the Miombo Ecosystem. In *Phenology and Seasonality Modeling*; Leith, H., Ed.; Springer: Berlin/Heidelberg, Germany, 1974; Volume 8.

43.   Kamutanda, D.K. *Evaluation des Éléments du Climat En R.D.C.*; Editions Universitaires Européenne: Saarbrücken, Allemagne, 2016.

44.   Baert, G.; van Ranst, E.; Ngongo, M.L.; Kasongo, E.L.; Verdoodt, A.; Mujinya, B.B.; Mukalay, J.M. *Guide des Sols en République Démocratique du Congo, Tome II: Description et Données Physico-Chimiques de Profils Types*; Ecole Technique Salama-Don Bosco: Lubumbashi, Congo, 2009; ISBN 978-90-76769-98-1.

45.   Gorelick, N.; Hancher, M.; Dixon, M.; Ilyushchenko, S.; Thau, D.; Moore, R. Google Earth Engine: Planetary-Scale Geospatial Analysis for Everyone. *Remote Sens. Environ.* **2017**, *202*, 18–27. [CrossRef]

46.   Phan, T.N.; Kuch, V.; Lehnert, L.W. Land Cover Classification Using Google Earth Engine and Random Forest Classifier—The Role of Image Composition. *Remote Sens.* **2020**, *12*, 2411. [CrossRef]

47.   Song, H.; Huang, B.; Liu, Q.; Zhang, K. Improving the Spatial Resolution of Landsat TM/ETM+ Through Fusion with SPOT5 Images via Learning-Based Super-Resolution. *IEEE Trans. Geosci. Remote Sens.* **2015**, *53*, 1195–1204. [CrossRef]

48.   Oszwald, J.; Lefebvre, A.; de Sartre, X.A.; Thales, M.; Gond, V. Analyse des directions de changement des états de surface végétaux pour renseigner la dynamique du front pionnier de Maçaranduba (Pará, Brésil) entre 1997 et 2006. *Teledetection* **2010**, *9*, 97–111.

49.   Zhao, Y.; An, R.; Xiong, N.; Ou, D.; Jiang, C. Spatio-Temporal Land-Use/Land-Cover Change Dynamics in Coastal Plains in Hangzhou Bay Area, China from 2009 to 2020 Using Google Earth Engine. *Land* **2021**, *10*, 1149. [CrossRef]

50.   Imam, E. *Remote Sensing and GIS Module: Colour Composite Images and Visual Image Interpretation*; University Grand Commission (UGC), Government of India: New Delhi, India, 2019.

51.   Imorou, I.T.; Arouna, O.; Zakari, S.; Djaouga, M.; Thomas, O.; Kinmadon, G. Des images satellites pour la gestion durable des territoires en Afrique. In Proceedings of the Actuellement au Bénin la Conférence OSFACO, Cotonou, Bénin, 13–15 March 2019; pp. 1–25.

52.　Breiman, L. Random Forests. *Mach. Learn.* **2001**, *45*, 5–32. [CrossRef]

53.　Svoboda, J.; Štych, P.; Laštovička, J.; Paluba, D.; Kobliuk, N. Random Forest Classification of Land Use, Land-Use Change and Forestry (LULUCF) Using Sentinel-2 Data—A Case Study of Czechia. *Remote Sens.* **2022**, *14*, 1189. [CrossRef]

54.　Mahdianpari, M.; Salehi, B.; Mohammadimanesh, F.; Motagh, M. Random Forest Wetland Classification Using ALOS-2 L-Band, RADARSAT-2 C-Band, and TerraSAR-X Imagery. *ISPRS J. Photogramm. Remote Sens.* **2017**, *130*, 13–31. [CrossRef]

55.　Xia, J.; Falco, N.; Benediktsson, J.; Du, P.; Chanussot, J. Hyperspectral Image Classification with Rotation Random Forest via KPCA. *IEEE J. Sel. Top. Appl. Earth Obs. Remote Sens.* **2017**, *10*, 1601–1609. [CrossRef]

56.　Cochran, W.G. *Sampling Techniques*; John Wiley and Sons: New York, NY, USA, 1977.

57.　Olofsson, P.; Foody, G.M.; Herold, M.; Stehman, S.V.; Woodcock, C.E.; Wulder, M.A. Good Practices for Estimating Area and Assessing Accuracy of Land Change. *Remote Sens. Environ.* **2014**, *148*, 42–57. [CrossRef]

58.　Pontius, R.G.; Millones, M. Death to Kappa: Birth of quantity disagreement and allocation disagreement for accuracy assessment. *Int. J. Remote Sens.* **2011**, *32*, 4407–4429. [CrossRef]

59.　Nelson, M.D.; Garner, J.D.; Tavernia, B.G.; Stehman, S.V.; Riemann, R.I.; Lister, A.J.; Perry, C.H. Assessing map accuracy from a suite of site-specific, non-site specific, and spatial distribution approaches. *Remote Sens. Environ.* **2021**, *260*, 112442. [CrossRef]

60.　Campbell, B.M. *The Miombo in Transition: Woodlands and Welfare in Africa*; Center for International Forestry Research: Bogor, Indonesia, 1996; ISBN 978-979-8764-07-3.

61.　Bogaert, J.; Ceulemans, R.; Salvador-Van Eysenrode, D. Decision Tree Algorithm for Detection of Spatial Processes in Landscape Transformation. *Environ. Manag.* **2004**, *33*, 62–73. [CrossRef]

62.　McGarigal, K. *FRAGSTATS Help*; University of Massachusetts: Amherst, MA, USA, 2015; p. 182. Available online: https://www.researchgate.net/profile/Samuel-Cushman-2/publication/259011515_FRAGSTATS_Spatial_pattern_analysis_program_for_categorical_maps/links/564217ea08aebaaea1f8b8dd/FRAGSTATS-Spatial-pattern-analysis-program-for-categorical-maps.pdf (accessed on 24 September 2023).

63.　Barima, Y.S.S.; Barbier, N.; Bamba, I.; Traoré, D.; Lejoly, J.; Bogaert, J. Dynamique paysagère en milieu de transition forêt-savane ivoirienne. *Bois Forêts Trop.* **2009**, *299*, 15. [CrossRef]

64.　Mama, A.; Sinsin, B.; Cannière, C.D.; Bogaert, J. Anthropisation et dynamique des paysages en zone soudanienne au nord du Bénin. *Tropicultura* **2013**, *11*, 78–88.

65.　Bogaert, J.; Barima, Y.S.S.; Ji, J.; Jiang, H.; Bamba, I.; Mongo, L.I.W.; Mama, A.; Nyssen, E.; Dahdouh-Guebas, F.; Koedam, N. A Methodological Framework to Quantify Anthropogenic Effects on Landscape Patterns. In *Landscape Ecology in Asian Cultures*; Hong, S.-K., Kim, J.-E., Wu, J., Nakagoshi, N., Eds.; Ecological Research Monographs; Springer: Tokyo, Japan, 2011; pp. 141–167. ISBN 978-4-431-87798-1.

66.　De Haulleville, T.; Rakotondrasoa, O.L.; Rakoto Ratsimba, H.; Bastin, J.-F.; Brostaux, Y.; Verheggen, F.J.; Rajoelison, G.L.; Malaisse, F.; Poncelet, M.; Haubruge, É.; et al. Fourteen Years of Anthropization Dynamics in the Uapaca Bojeri Baill. Forest of Madagascar. *Landsc. Ecol. Eng.* **2018**, *14*, 135–146. [CrossRef]

67.　Warrens, M.J. Properties of quantity disagreement and the allocation disagreement. *Int. J. Remote Sens.* **2015**, *36*, 1439–1446. [CrossRef]

68.　Useni, S.Y.; Cabala, K.S.; Nkuku, K.C.; Amisi, M.Y.; Malaisse, F.; Bogaert, J.; Munyemba, K.F. Vingt-cinq ans de monitoring de la dynamique spatiale des espaces verts en réponse à l'urbanisation dans les communes de la ville de Lubumbashi (Haut-Katanga, R.D. Congo). *Tropicultura* **2017**, *35*, 300–311.

69.　Mwanga, E.O.; Mwanga, M.O. Socio-economic factors driving deforestation in Katanga Province, southeastern region of the Democratic Republic of Congo. *Afr. J. Environ. Sci. Technol.* **2017**, *11*, 141–150.

70.　Karsenty, A.; Ongolo, S. Timber production in the Congo Basin: Challenges and perspectives. *Forests* **2019**, *10*, 303.

71.　Matavire, M.M.; Sibanda, M.; Dube, T. Assessing the Aftermath of the Fast Track Land Reform Programme in Zimbabwe on Land-Use and Land-Cover Changes. *Trans. R. Soc. S. Afr.* **2015**, *70*, 181–186. [CrossRef]

72.　Dibwe, M.D. *Lubumbashi, Ville Industrielle Attractive et Repulsive (1910–2008)*; Los Restos de la Pobreza Urbana: Madrid, Spain, 2009.

73.　Trefon, T.; Hendriks, T.; Kabuyaya, N.; Ngoy, B. *L'économie Politique de la Filière du Charbon de Bois à Kinshasa et à Lubumbashi. Appuis Stratégique à la Politique de la Reconstruction Post-Conflit en R.D.C.*; Working paper of the Institute of Development Policy and Management; University of Antwerp: Antwerp, Belgium, 2010.

74.　Chidumayo, E.N. Is Charcoal Production in Brachystegia-Julbernardia Woodlands of Zambia Sustainable? *Biomass Bioenergy* **2019**, *125*, 1–7. [CrossRef]

75.　Sedano, F.; Silva, J.A.; Machoco, R.; Meque, C.H.; Sitoe, A.; Ribeiro, N.; Anderson, K.; Ombe, Z.A.; Baule, S.H.; Tucker, C.J. The Impact of Charcoal Production on Forest Degradation: A Case Study in Tete, Mozambique. *Environ. Res. Lett.* **2016**, *11*, 094020. [CrossRef]

76.　Mertens, B.; Lambin, E.F. Land-Cover-Change Trajectories in Southern Cameroon. *Ann. Assoc. Am. Geogr.* **2000**, *90*, 467–494. [CrossRef]

77.　Zézouma, S.; Mipro, H.; Boalidioa, T.; Martin, K.; Irenée, S. Impact des villages et du réseau routier sur la structure spatiale de la forêt classée de Koulbi (Sud-Ouest du Burkina Faso). *Sci. Nat. Appl.* **2019**, *38*, 652.

78.　Battisti, C.; Contoli, L. Diversity Indices as 'Magic' Tools in Landscape Planning: A Cautionary Note on Their Uncritical Use. *Landsc. Res.* **2011**, *36*, 111–117. [CrossRef]

79. De Mufuta, N.J.D.; Omari, M.F.; Banza, W.I.R.; Ngasa, M.P. Les Entités Territoriales Décentralisées(ETD) Face à La Redevance Minière. Politiques Économiques et Gouvernance Des Ressources Naturelles En République Démocratique Du Congo. *Rev. Française D'economie Gest.* **2022**, *3*, 482–501.

80. De Wasseige, C.; Flynn, J.; Louppe, D.; Hiol Hiol, F.; Mayaux, P. *Les Forêts du Bassin du Congo—Etat des Forêts 2013*; Weyrich: Neufchâteau, Belgique, 2014; ISBN 978-2-87489-298-1.

81. Mputu, E.K.; Kabongo, J.M.; Muilu, M. Industrie minière et développement socio-économique local: Regard sur Fungurume dans le Katanga (Sud-Est de la RD Congo). *Int. J. Innov. Apply Stud.* **2019**, *27*, 728–741.

82. Maréchal, J.; Useni, S.Y.; Bogaert, J.; Munyemba, K.F.; Mahy, G. La perception par des experts locaux des espaces verts et de leurs services écosystémiques dans une ville tropicale en expansion: Le cas de Lubumbashi. In *Anthropisation des Paysages Katangais*; Bogaert, J., Colinet, G., Mahy, G., Eds.; Presses Universitaires de Liège: Liège, Belgique, 2018; pp. 59–69.

83. Hick, A.; Hallin, M.; Tshibungu, A.; Mahy, G. La place de l'arbre dans les systèmes agricoles de la région de Lubumbashi. In *Anthropisation des Paysages Katangais*; Bogaert, J., Colinet, G., Mahy, G., Eds.; Les Presses Universitaires de Liège—Agronomie: Gembloux, Belgium, 2018; pp. 111–123.

84. Biloso, A.; Lejoly, J. Etude de l'exploitation et Du Marché Des Produits Forestiers Non Ligneux à Kinshasa. *Tropicultura* **2006**, *24*, 183–188.

85. Loubelo, E. Impact des Produits Forestiers non Ligneux (PFNL) sur L'économie des Ménages et la Sécurité Alimentaire: Cas de la République du Congo. Ph.D. Thesis, Université Rennes 2, Rennes, France, 2012.

86. Péroches, A.; Nge, O.A.; Gazull, L.; Dubliez, E. *Programme de Consommation Durable et Substitution Partielle Au Bois-Énergie*; Rapport d'étude Sur La Filière Bois-Énergie de La Ville de Lubumbashi; CIRAD: Montpellier, France, 2021.

87. Chidumayo, E.N.; Gumbo, D.J. The Environmental Impacts of Charcoal Production in Tropical Ecosystems of the World: A Synthesis. *Energy Sustain. Dev.* **2013**, *17*, 86–94. [CrossRef]

88. Maindo, A.; Kapa, F. *La Foresterie Communautaire en RDC*; Tropenbos International RD Congo: Kisangani, Congo, 2014.

89. Kyalamakasa, J.M.K.; Mulambi, M.M.M.; Mukonzo, E.K.L.; Shutcha, M.N.; Tekeu, H.; Nkombe, A.K.; Khasa, D. Early Selection of Tree Species for Regeneration in Degraded Woodland of Southeastern Congo Basin. *Forests* **2021**, *12*, 117. [CrossRef]

90. Vroh, B.T.A.; Kone, Y. Valeur écologique et produits de cueillette des plantations forestières de la Forêt classée de la Téné. *Vertigo* **2021**, *21*, 32783. [CrossRef]

91. Sileshi, G.; Akinnifesi, F.K.; Ajayi, O.C.; Chakeredza, S.; Kaonga, M.; Matakala, P.W. Contributions of Agroforestry to Ecosystem Services in the Miombo Eco-Region of Eastern and Southern Africa. *Afr. J. Environ. Sci. Technol.* **2007**, *1*, 68–80.

92. Kimaro, A.A.; Isaac, M.E.; Chamshama, S.A.O. Carbon Pools in Tree Biomass and Soils Under Rotational Woodlot Systems in Eastern Tanzania. In *Carbon Sequestration Potential of Agroforestry Systems: Opportunities and Challenges*; Kumar, B.M., Nair, P.K.R., Eds.; Advances in Agroforestry; Springer: Dordrecht, The Netherlands, 2011; pp. 129–143. ISBN 978-94-007-1630-8.

93. Yabi, J.A.; Bachabi, F.X.; Labiyi, I.A.; Ode, C.A.; Ayena, R.L. Déterminants socio-économiques de l'adoption des pratiques culturales de gestion de la fertilité des sols utilisées dans la commune de Ouaké au Nord-Ouest du Bénin. *Int. J. Biol. Chem. Sci.* **2016**, *10*, 779. [CrossRef]

94. Kitoto, P.A.O. Facteurs d'adoption des foyers améliorés en milieux urbains sahéliens camerounais. *Économie Géographie Polit. Droit Social.* **2018**, *9*, 12182. [CrossRef]